# 宇宙空間光通信用 連続波単一横モード偏波保持 10 W Er/Yb 共添加ファイバー増幅器の開発

小林啓紀，狩野良子，瀬尾崇志，鈴木康史，水田栄一，橋本洋輔，荒木智宏，高田康利

# Development of a Continuous Wave Single Transverse Mode Polarization-Maintaining 10 W Er/Yb-Codoped Fiber Amplifier for Space Communications†

Hiroki KOBAYASHI, Ryoko KANO, Takashi SEO, Yasushi SUZUKI, Eiichi MIZUTA, Yosuke HASHIMOTO, Tomohiro ARAKI and Yasutoshi TAKADA

宇宙空間でのデータ通信量の増加に伴い，宇宙空間光通信への注目が高まっている．ニコンと JAXA は，大容量宇宙光ネットワーク開発の一環として，変調連続波信号用の単一横モード動作，10 W 偏波保持 Er/Yb 共添加ファイバー (EYDF) 増幅器の開発を進めてきた．現在，エンジニアリングモデル（EM）の開発を完了し，2024年に国際宇宙ステーションにて，光通信実証実験を行う予定である．

光増幅器は，耐放射線性 EYDF を用いた 3 段の後方励起構成からなる．励起用レーザーダイオードと寄生発振防止のためのモニター用フォトダイオードを備え，いずれも十分な放射線耐性を確認した．また，制御基板も含んでいる．外形寸法は，300 mm× 380 mm× 76 mm，重さは 6.3 kg であった．

室温大気圧下，−3 dBm の信号光入力時に，合計 34 W 励起で 10 W の光出力を得，ウォールプラグ効率10.1% を達成した．また，室温大気圧下で，出力光量 10 W，2000時間の動作を達成した．

宇宙用コンポーネントとしての信頼性を確保するため，振動試験と熱真空試験を実施した．動作温度範囲の上下端，± 0℃と +50℃で，出力光量 10 W，偏光消光比（PER）16 dB 以上を達成し，性能劣化は認められなかった．

Space optical communications have attracted growing attention as space data traffic volumes continue to increase, and as part of ongoing efforts to develop high-speed optical space networks, Nikon and JAXA have been developing a single-transverse-mode 10 W polarization-maintaining Er/Yb-codoped fiber (EYDF) amplifier for modulated continuous-wave signals. We have finished developing the engineering model (EM) and plan to demonstrate this amplifier as a part of optical communication system on the International Space Station in 2024.

The EM amplifier has a three-stage backward pumping structure with radiation-hardened EYDF. It also includes pump laser diodes, and power monitoring photodiodes to avoid parasitic lasing, both of which have been confirmed to have adequate radiation tolerance, as well as a control driver circuits. The overall dimensions are 300 mm × 380 mm × 76 mm, and it weighs 6.3 kg.

The EM amplifier achieved optical output power of 10 W at pumping power of 34 W in total under standard temperature and pressure conditions (STP: room temperature, 1 atm) with a −3 dBm signal input. The total wall-plug efficiency reached 10.1%. The amplifier achieved an operating time of 2000 hours at 10 W under STP.

We conducted a mechanical vibration test and an operating thermal vacuum test to ensure the reliability of the amplifier as a space component. At the upper and lower end of the operation temperature range, ± 0 and +50°C, the output power and polarization extinction ratio (PER) were > 10 W and > 16 dB, respectively, without any degradation of the amplification gain or PER.

**Key words** 自由空間光通信，高出力光ファイバー増幅器，宇宙運用，真空，放射線耐性
free space optical communications, high power fiber amplifiers, space operations, vacuum, radiation tolerance

## 1 Introduction

The volume of data traffic in space communications continues to increase. However, the channel capacity of conventional radio waves is reaching to its limit, and the carrier frequency has been extended to millimeter-wave band.

Free-space optical communications have attracted attention in recent years as a means of exceeding this limitation

† This paper is reprinted with permission from SPIE, the international society for optics and photonics [6].

by increasing the carrier frequency dramatically. In 1994, the Communications Research Laboratory (CRL, now the National Institute of Information and Communications Technology, NICT) in Japan achieved the first ground-to-space optical communication using the Laser Communication Equipment (LCE) on ETS-VI [1], which was developed and launched by the National Space Development Agency (NASDA, now part of JAXA). Following that, the European Space Agency (ESA) achieved the first space-to-space optical communication between SPOT-4 and ARTEMIS in 2001 [2]. JAXA and ESA also achieved the first space-to-space bi-directional optical communication link between OICETS and ARTEMIS in 2005 [3].

Since these demonstrations were in the early days of free-space optical communications, the signals were transmitted by 0.8 μm laser diodes (LDs) using the intensity modulation-direct detection (IM-DD) method [4]. The data transfer rate limitation can be increased by applying advanced modulation methods, such as phase-shift keying, compared with IM-DD.

Today, data transfer rates on the ground have exceeded 100 Gbit/(s·fiber). Our goal is for the space-based backbone network to communicate as rapidly as ground-based optical communications, and the optical high-power amplifier (OHPA) is one of the key components.

JAXA is developing an optical data relay system named "LUCAS," which stands for the Laser Utilizing Communication System [5]. To promote faster communication with smaller size, weight, and power (SWaP) optical communication terminals in the near future, compared with the present LUCAS, we began to develop a 10 W OHPA and to install and evaluate it on the International Space Station (ISS). In this article, we provide details of the developed engineering model (EM), which was used to evaluate the environmental tolerances required in order to advance to the proto-flight model (PFM) to be launched.

## 2 Amplifier Design

To achieve the aims described above, we designed the amplifier as follows.

### 2.1. Target Specification

We set the target specifications as shown in Table 1, with reference to the overall system requirements and the ISS Japanese Experiment Module (JEM) interface specifications.

### 2.2. System Structure

The amplifier contains the optical fiber amplifiers and the electrical control driver board in a single package (Fig. 1). The PDs monitor the optical power and protect the amplifier by detecting anomalies such as parasitic lasing.

### 2.3. Amplifier Optical Structure

The amplifier has three stages of Er/Yb-codoped fibers (EYDFs) (Fig. 2). All of these stages have backward pumping configurations. The passive optical components, the LDs, and the photodiodes (PDs) are commercial off-the-shelf (COTS) products. The radiation tolerances of the EYDFs were confirmed by the manufacturer. The booster LDs (#2 & #3) are driven together by one control driver.

Table 1 Target specifications for evaluation on the ISS and actual measured values of the OHPA

| Item | | Unit | Target specification | Achieved value |
|---|---|---|---|---|
| Input optical power level | | dBm | −3.0 to +3.0 | |
| Output optical power level | | dBm | > +40.0 | > +40.0 |
| Optical power gain | | dB | 37 to 43 | |
| Signal wavelength | | nm | 1560.606 | |
| Signal modulation | | — | RZ-DPSK | |
| Modulation rate | | GHz | > 2.5 | |
| Polarization extinction ratio (PER) | | dB | > 15 | > 16 |
| Return light at 10 W operation | | dBm | < −39 | < −45 |
| Total power consumption (EOL at 25°C, see §5) | | W | < 151 | 103 |
| Wall-plug efficiency (EOL at 25°C, see §5) | | — | > 8% | 9.7% |
| Storage temperature | | °C | −40 to +70 | |
| Operating temperature | | °C | ± 0 to +50 | |
| Dimensions (Protrusions not included) | Width | mm | < 360 | 300 |
| | Depth | mm | < 300 | 300 |
| | Height | mm | < 100 | 76 |
| Weight | | kg | < 7.0 | 6.3 |
| Operating period | | year | > 3 | |
| Operating duty | | — | 5% | |

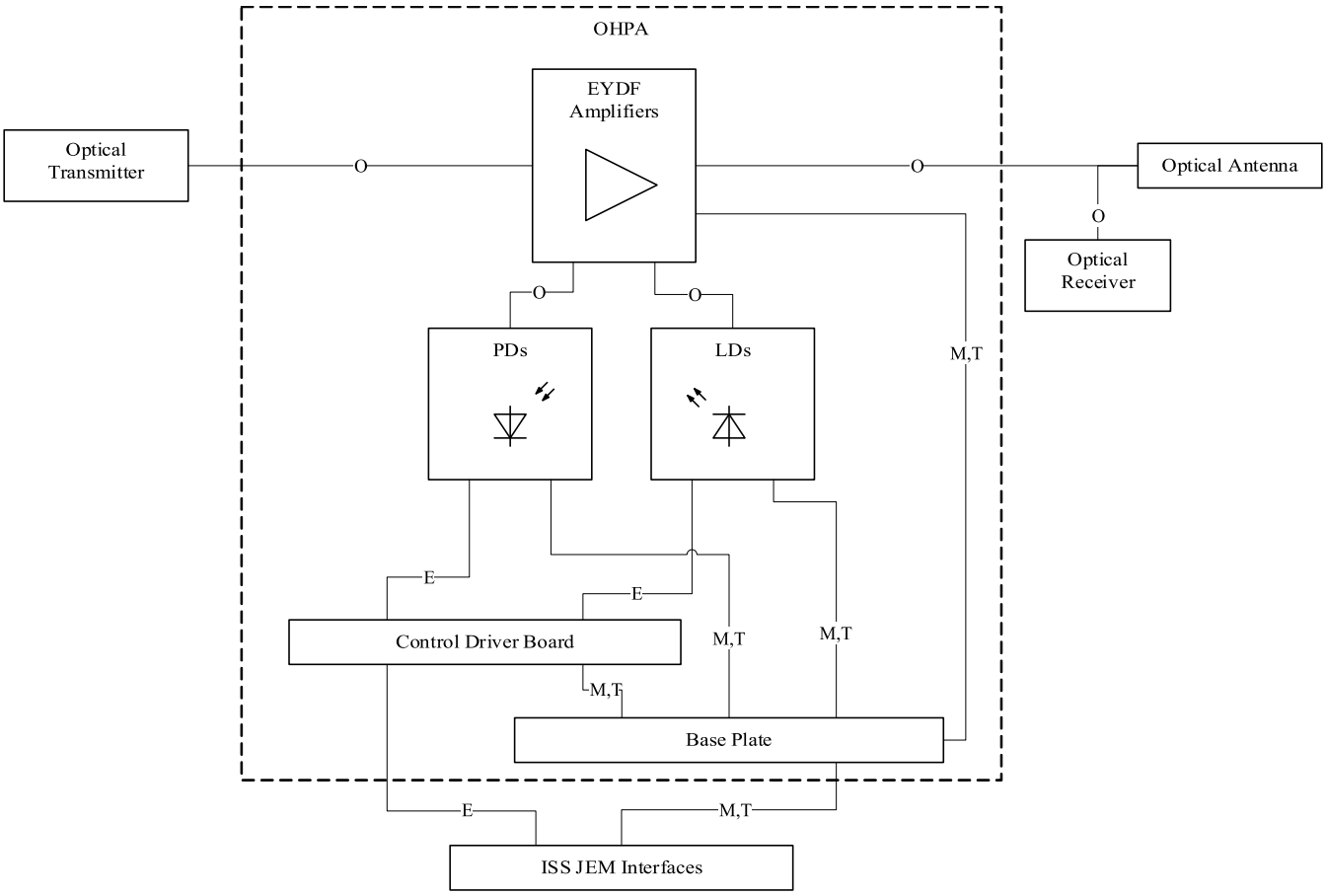


Fig. 1 System block diagram of the optical transceiver: the letter symbols on the connecting lines represents, the electrical (E), mechanical (M), optical (O), and thermal (T) interfaces.

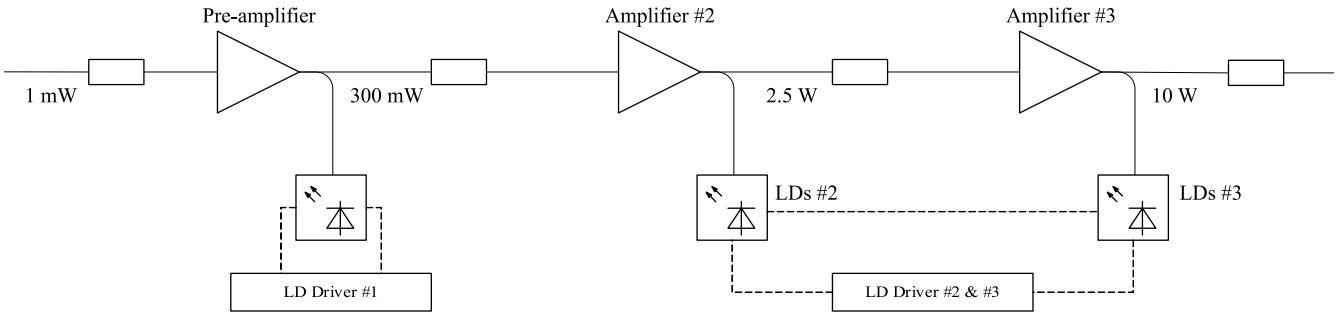


Fig. 2 Optical block diagram

### 2.4. Mechanical and Electrical Design

The total dimensions of the amplifier are 300 mm × 380 mm × 76 mm, and its appearance is shown in Fig. 3. The amplifier weighs 6.3 kg, including the control driver board and the electrical components. It has one optical connector for the input signals, one optical output pigtail, and 3 electrical connectors for a DC 28 V power supply and telemetry & command communications.

Fig. 3 Appearance of the amplifier

## 3 Radiation Tolerance of Semiconductor Components

### 3.1. Radiation Dose Condition

To ensure radiation tolerance, experiments were conducted in which radiation was applied to the semiconductor electro-optical (e-o) components.

Table 2 describes the radiation dose conditions for the ISS experiment, assuming 1 year of operation on the ISS with a 50% margin. Table 3 describes more severe conditions, which anticipate future changes in operating conditions, such as 10 years of operation in geostationary orbit (GEO).

The tests confirmed that the changes in the characteristics were sufficiently small for the target operating period of the amplifier (see §5).

### 3.2. LDs Exposed to Gamma Ray Radiation

Four samples of the same LD products were irradiated with gamma rays. The results in Fig. 4 shows output power degradations of < 2.8% and < 4.7% at exposures of 30 Gy and 1000 Gy, respectively.

### 3.3. LDs Exposed to Proton Radiation

Four samples of the same LD products were irradiated with protons. The results in Fig. 5 show output power degradations of < 0.8% and < 1.4% at exposures of $1.5 \times 10^9$ $p^+/cm^2$ and $1.0 \times 10^{11}$ $p^+/cm^2$, respectively.

### 3.4. PDs Exposed to Gamma Ray Radiation

The measurement was conducted at the same time as the experiment described in §3.2. Four samples of the same PD products were irradiated with gamma rays. The results in Fig. 6 show e-o conversion efficiency decreases of < 1.3% and < 1.3% at exposures of 30 Gy and 1000 Gy, respectively.

### 3.5. PDs Exposed to Proton Radiation

Four of the same PD products were irradiated with protons at the same time as the experiment described in §3.3. The results in Fig. 7 show the e-o conversion efficiency decrease of almost 0% and < 4.9% at exposures of $1.5 \times 10^9$ $p^+/cm^2$ and $1.0 \times 10^{11}$ $p^+/cm^2$, respectively.

## 4 Test Results for the OHPA

### 4.1. Optical Output Power under STP

The amplifier emitted output power of 10 W with a −3 dBm input and a total booster pumping power of 31.5 W under standard temperature and pressure (STP: room temperature, 1 atm) (Fig. 8). The input signal was a 1.5 μm continuous-wave (CW), and the linewidth was ~5 GHz. The pumping power for the preamplifier was fixed to 2.3 W. The total power pumping of the LDs was 33.7 W, which means the total (from the preamplifier to the booster amplifiers) optical-optical (o-o) conversion efficiency was 29.7%.

Table 2 Radiation dose conditions for the ISS experiment

| Type | Energy | Flux | Fluence |
|---|---|---|---|
| Protons ($p^+$) | 70 MeV | $1.0 \times 10^7$ $p^+/(cm^2 \cdot s)$ | $1.5 \times 10^9$ $p^+/cm^2$ |
| Gamma rays ($^{60}Co$) | 1.17 & 1.33 MeV | 62 Gy/h | 30 Gy |

Table 3 Radiation dose conditions for future plans with more severe conditions

| Type | Energy | Flux | Fluence |
|---|---|---|---|
| Protons ($p^+$) | 70 MeV | $1.0 \times 10^8$ $p^+/(cm^2 \cdot s)$ | $1.0 \times 10^{11}$ $p^+/cm^2$ |
| Gamma rays ($^{60}Co$) | 1.17 & 1.33 MeV | 225 Gy/h | 1000 Gy |

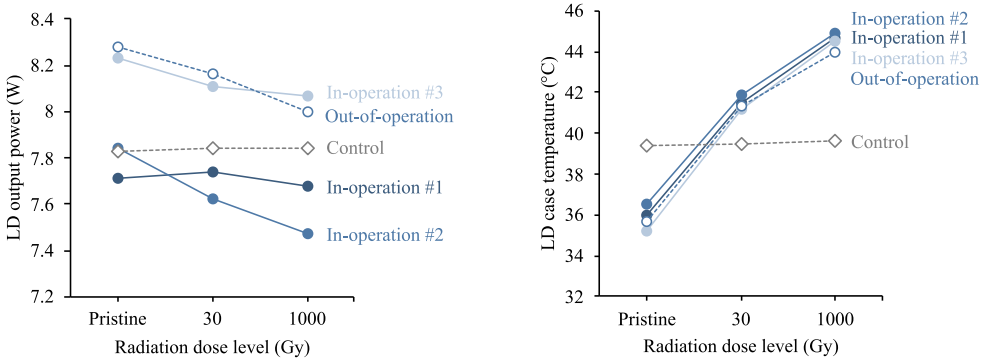


Fig. 4 Output power at 9.0 A operation versus radiation dose (left) and LD case temperature versus radiation dose (right): three in-operation samples (filled blue circles), one out-of-operation sample (open blue circle), and one non-irradiated control sample (open gray diamond)

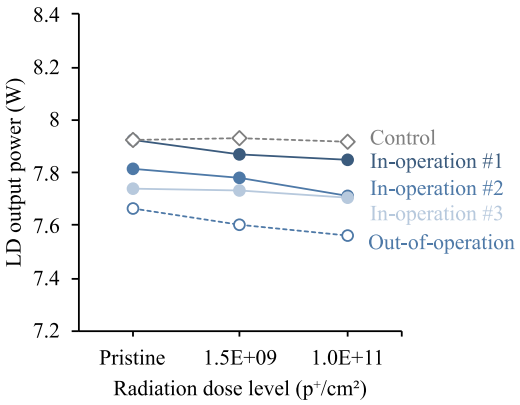


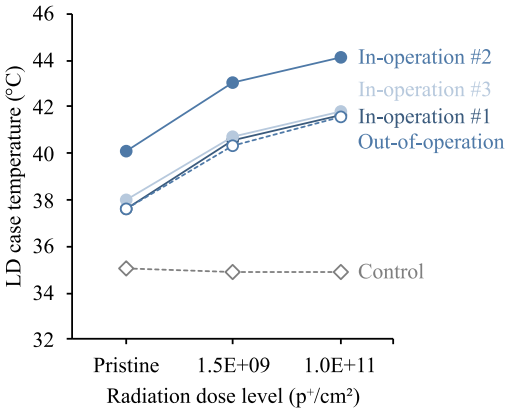


Fig. 5 Output power at 9.0 A operation versus radiation dose (left) and LD case temperature versus radiation dose (right): three in-operation samples (filled blue circles), one out-of-operation sample (open blue circle), and one non-irradiated control sample (open gray diamond)

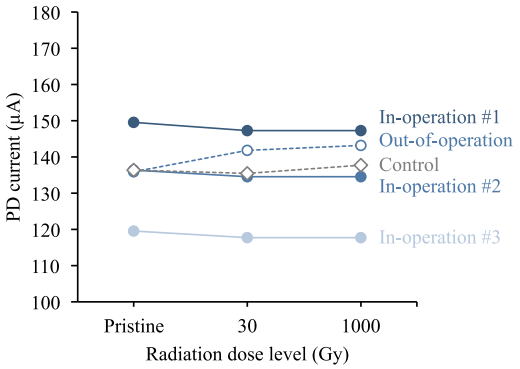


Fig. 6 Output power at 150 μW input versus radiation dose: three in-operation samples (filled blue circles), one out-of-operation sample (open blue circle), and one non-irradiated control sample (open gray diamond)

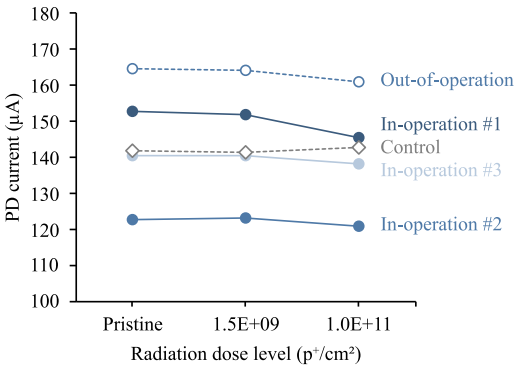


Fig. 7 Output current at 150 μW input versus radiation dose three in-operation samples (filled blue circles), one out-of-operation sample (open blue circle), and one non-irradiated control sample (open gray diamond)

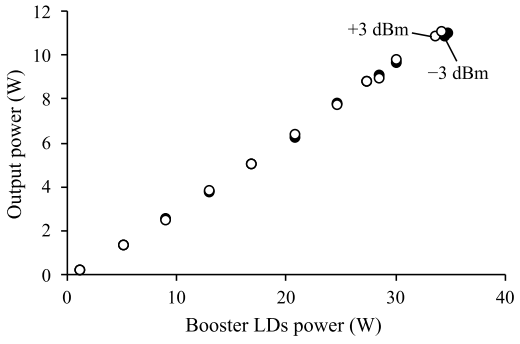


Fig. 8 Output power versus pumping power for inputs of −3 dBm (filled) and +3 dBm (open)

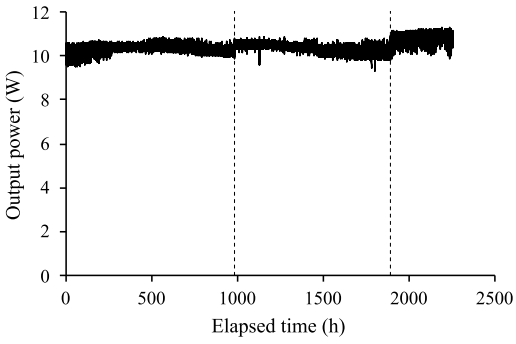


Fig. 9 Output power (solid line) versus elapsed time: at elapsed times of 990 and 1870 hours (dashed line), the amplifier was restarted.

### 4.2. Energy Conversion Efficiency

The estimated energy conversion efficiency at each part of the amplifier at output power of 10 W is shown in Table 4. The amplifier achieved a total wall-plug efficiency of 10.1% measured at 10.8 W operation under STP.

### 4.3. Long-Term Operation under STP

Under STP, long-term operation was applied to an experimental model of the amplifier, which has the same optical structure as the one described in §4.1. No power degradation was observed (Fig. 9). This indicates that the photodarkening effect was sufficiently small. Additionally, although the input signal had high coherence, this caused

Table 4 Estimated energy conversion efficiency at each part of the amplifier under STP: the total input power consists of the items shown in bold. Upright: electrical power; italic: optical power

| Item | Input (W) | Output (W) | Efficiency | Consumption (W) |
|---|---|---|---|---|
| **LD driver #1** | 0.4 | — | — | 0.4 |
| **LD #1 DC-DC** | 5.9 | 4.2 | 71.3% | 1.7 |
| LD #1 e-o | 4.2 | *2.2* | 52.9% | 2.0 |
| Preamplifier o-o | *2.2* | *0.3* | 12.9% | 1.9 |
| **LD driver #2 & #3** | 11.4 | — | — | 11.4 |
| **LD #2 & #3 DC-DC** | 75.0 | 54.8 | 73.0% | 20.2 |
| LD #2 & #3 total e-o | 54.8 | *31.5* | 57.5% | 23.3 |
| Booster amplifiers #2 & #3 o-o | *31.5* | *10.0* | 31.8% | 21.5 |
| **Other electrical components** | 5.4 | — | — | 5.4 |
| **Total wall-plug efficiency** | **98.1** | ***10.0*** | **10.1%** | **88.1** |

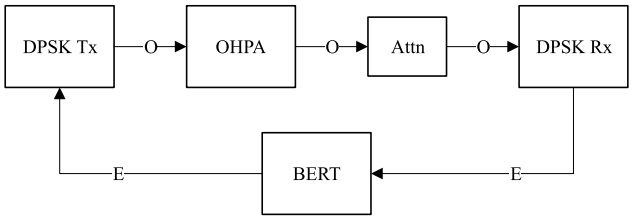


Fig. 10 Communication test system setup: DPSK Tx: DPSK transmitter, Attn: optical attenuator, DPSK Rx: DPSK receiver, and BERT: bit-error-rate tester

Table 5 Communication test conditions.

| Item | Value |
|---|---|
| Modulation method | DPSK (RZ-33%) |
| Transfer rate | 2.5 Gbps |
| Signal pattern | PRBS $2^{15}-1$ |

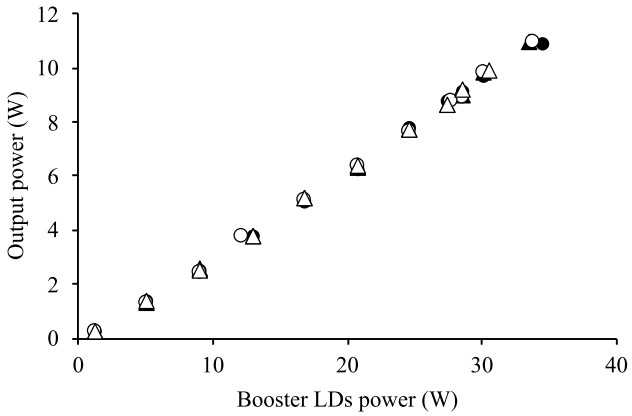


Fig. 11 Output power versus pumping power: before excitation (filled circle), and after *z*-axis (filled triangle), *x*-axis (open circle), and *y*-axis (open triangle) excitation

almost no higher-order transverse mode instability (HOMI), and no power degradation.

### 4.4. Communication Test

The amplifier was subjected to a communication test with the setup shown in Fig. 10 and conditions shown in Table 5. No error was observed throughout 30 s measurement duration, and it shows that the bit-error-rate (BER) value was below $4 \times 10^{-11}$ with the 95% confidence level.

### 4.5. Vibration Test

The amplifier was subjected to a vibration test in the order of *z*-axis, *x*-axis, and *y*-axis excitation (Fig. 12). Almost no power degradation was observed (−0.5% as a measured value) throughout the three-axis test (Fig. 11).

### 4.6. Thermal Vacuum Test

The amplifier was subjected to a thermal vacuum test (Fig. 13) followed by the vibration tests. The test sequence is shown in Fig. 14. During the cycle #1, some function checks with turn-on and turn-off were performed. The temperature range was set to ± 0 to +56°C, taking into account the test margin. Throughout the test, the atmospheric pressure was maintained at $< 1.3 \times 10^{-3}$ Pa.

There was an 8% power degradation observed after vacuuming (Fig. 15). At +56°C, the slope efficiency decreased 12% compared with that at +25°C, while at ± 0°C, the efficiency increased 2%. The change between the initial and post-test measurements was caused by temperature difference. As the OHPA reached the temperature equilibrium, the output power returned. The amplifier emitted over 8.7 W throughout the test in the temperature range of ± 0 to +56°C (Fig. 16). The PER values at ± 0 and +56°C were > 16 dB (Fig. 17). The power limitation was caused by the temperature of the booster LDs becoming higher than the set upper limit, due to the large thermal resistance and temperature variation of the vacuum chamber. In the operating temperature range of ± 0 to +50°C, however, the amplifier emitted > 10 W.

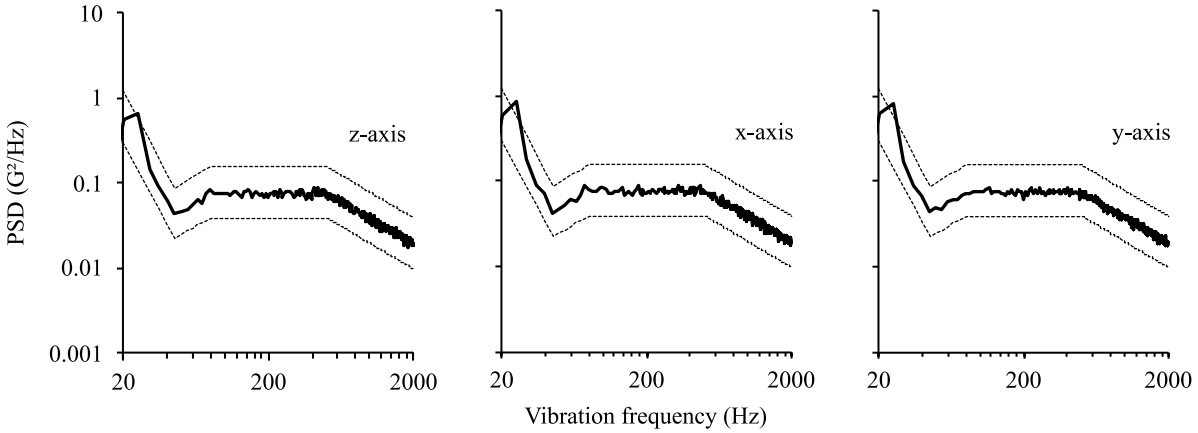


Fig. 12 Power spectral density (PSD) versus vibration frequency: measured values (bold solid) and target conditions ± 3 dB (thin dashed)

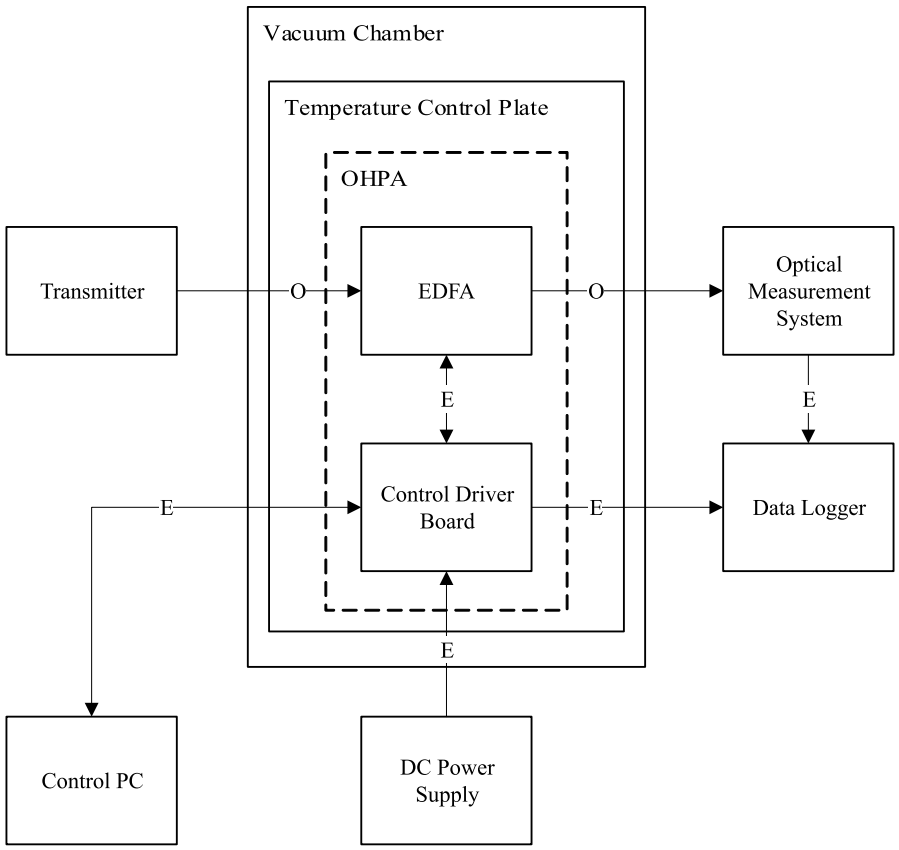


Fig. 13 Setup for the thermal vacuum test

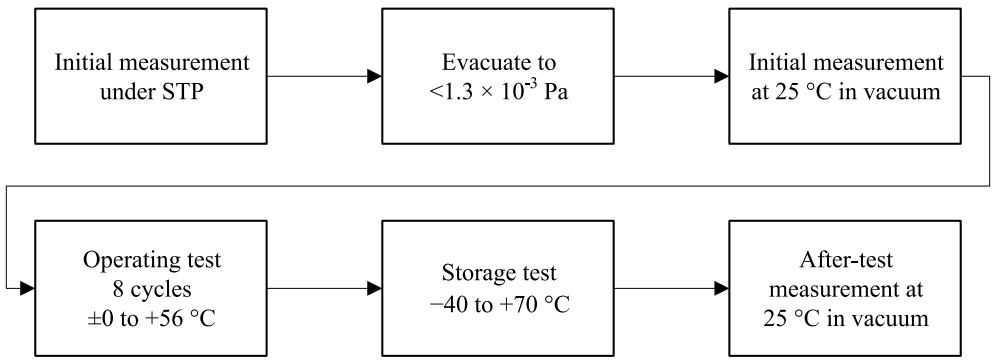


Fig. 14 Test sequence for the thermal vacuum test

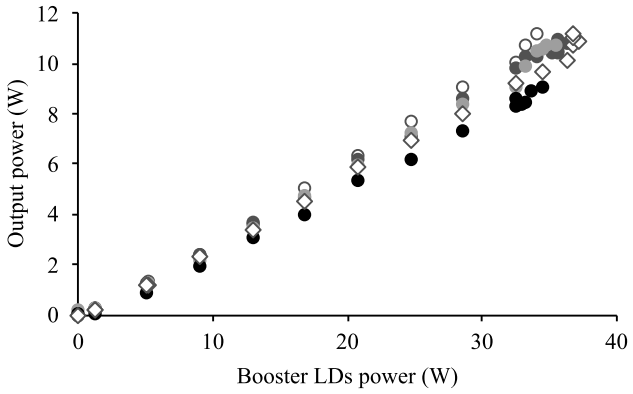


Fig. 15 Output power versus pumping power: initial measurement under STP (open dark gray circle), initial measurement at +25°C in vacuum (filled dark gray circle), ± 0°C in vacuum (filled light gray circle), and +56°C in vacuum (filled black circle), and post-test measurement at +25°C in vacuum (open dark gray diamond)

In the next step, development of the PFM, we plan to revise the design and evaluation setup to improve the thermal conductivity, thereby suppressing the temperature of the LDs.

## 5 Estimated End-of-Life (EOL) Characteristics

The target lifetime of the OHPA is 1500 hours of operation (Table 1). We estimated the EOL characteristics at 25°C of the amplifier. The estimated total wall-plug efficiency was 9.7% and the output decrease factor was expanded, as shown in Table 6.

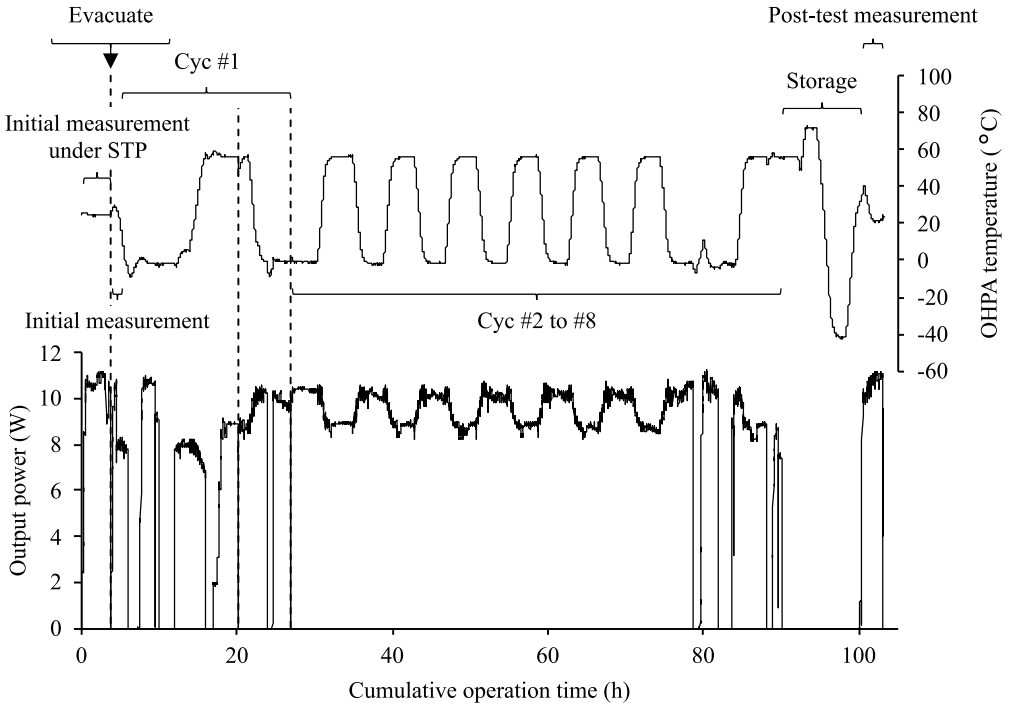


Fig. 16 Optical output power and temperature profiles throughout the test: the dashed lines show suspensions.

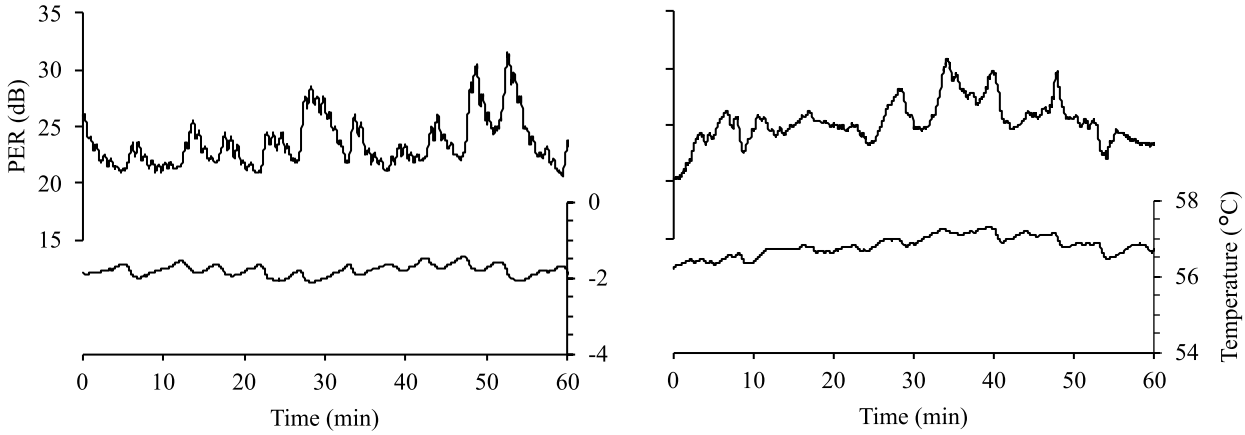


Fig. 17 PER and OHPA temperature time transitions at ± 0 (left) and +56°C (right)

Table 6 Output decrease factors, BOL and EOL specifications, and decrease rates

| Input | BOL | EOL | Difference |
|---|---|---|---|
| LD #1 e-o | 52.9% | 51.0% | −1.9 pp |
| Preamplifier o-o | 12.9% | 12.7% | −0.2 pp |
| LD #2 & #3 total e-o | 57.5% | 55.6% | −1.9 pp |
| Booster amplifiers #2 & #3 o-o | 31.8% | 31.3% | −0.5 pp |
| Other electrical components | 12.0 W | 13.2 W | +1.2 W |
| **Total wall-plug efficiency** | **10.1%** | **9.7%** | **−0.4 pp** |

## 6 Conclusion

We have described our CW single-transverse-mode polarization-maintaining 10 W EYDF amplifier.

The beginning-of-life (BOL) power consumption was 98.1 W at an optical output power of 10 W. The LDs and PDs were subjected to radiation tests, and < 4.7% power degradation of the LDs and almost no changes in the e-o characteristics of the PDs were observed. The amplifier was also subjected to vibration and thermal vacuum tests, and no power degradations were observed. These degradations had little influence on the amplifier's performance. Due to undesirable thermal conditions in the vacuum chamber, the output power was limited to 8.7 W at +56°C, but in the operating temperature range, the amplifier emitted > 10 W. The estimated EOL (1500 hours) power consumption was 102.9 W and the total wall-plug efficiency was 9.7%.

**Acknowledgment.** The authors would like to thank everyone involved in this work at Nikon and JAXA. Furthermore, support for the communication test from the Human Spaceflight Technology Center, Human Spaceflight Technology Directorate, JAXA, is greatly appreciated.

## References

[1] K. Araki, Y. Arimoto, M. Shikatani, M. Toyoda, M. Toyoshima, T. Takahashi, S. Kanda, and K. Shiratama, "Performance evaluation of laser communication equipment onboard the ETS-VI satellite," in *Proc. SPIE* 2699*, Free-Space Laser Communication Technologies VIII*, 1996.

[2] Z. Sodnik, B. Furch, and H. Lutz, "Optical intersatellite communication," *IEEE Journal of Selected Topics in Quantum Electronics,* vol. 16, no. 5, pp. 1051–1057, 2010.

[3] T. Jono, Y. Takayama, K. Shiratama, I. Mase, B. Demelenne, Z. Sodnik, A. Bird, M. Toyoshima, H. Kunimori, D. Giggenbach, N. Perlot, M. Knapek, and K. Arai, "Overview of the inter-orbit and the orbit-to-ground laser communication demonstration by OICETS," in *Proc. SPIE* 6457*, Free-Space Laser Communication Technologies XIX and Atmospheric Propagation of Electromagnetic Waves*, 2007.

[4] T. Araki, "Research and development trends of space optical communications for realizing large capacity communication," *IEICE Communications Society Magazine,* vol. 13, no. 3, pp. 205–215, 2019.

[5] S. Yamakawa, Y. Satoh, T. Itahashi, Y. Takano, S. Hoshi, Y. Miyamoto, M. Sugiho, T. Yoshizawa, Y. Koizumi, M. Yukizane, S. Suzuki, and H. Kohata, "LUCAS: The second-generation GEO satellite-based space data-relay system using optical link," in 2022 *IEEE International Conference on Space Optical Systems and Applications (ICSOS)*, 2022.

[6] H. Kobayashi, R. Kano, T. Seo, Y. Suzuki, E. Mizuta, Y. Hashimoto, T. Araki, and Y. Takada, "Development of a continuous wave single transverse mode polarization-maintaining 10 W Er/Yb-codoped fiber amplifier for space communications," in *Proc. SPIE* 12413*, Free-Space Laser Communications XXXV*, 2023.

小林啓紀　Hiroki KOBAYASHI
先進技術開発本部 光デバイス開発センター
Opto Device Development Center
Advanced Technology Research & Development Division

狩野良子　Ryoko KANO
精機事業本部 半導体装置事業部 開発統括部 第一開発部
1st Development Department
Development Sector
Semiconductor Lithography Business Unit
Precision Equipment Group

瀬尾崇志　Takashi SEO
先進技術開発本部 光デバイス開発センター
Opto Device Development Center
Advanced Technology Research & Development Division

鈴木康史　Yasushi SUZUKI
カスタムプロダクツ事業部 開発部
Development Department
Customized Products Business Unit

水田栄一　Eiichi MIZUTA
宇宙航空研究開発機構
Japan Aerospace Exploration Agency

橋本洋輔　Yosuke HASHIMOTO
宇宙航空研究開発機構
Japan Aerospace Exploration Agency

荒木智宏　Tomohiro ARAKI
宇宙航空研究開発機構
Japan Aerospace Exploration Agency

高田康利　Yasutoshi TAKADA
先進技術開発本部 光デバイス開発センター
Opto Device Development Center
Advanced Technology Research & Development Division